

Evidence for High Energy Resummation Effects in Mueller-Navelet Jets at the LHC

B. Ducloué,¹ L. Szymanowski,² and S. Wallon^{1,3}

¹*LPT, Université Paris-Sud, CNRS, 91405 Orsay, France*

²*National Centre for Nuclear Research (NCBJ), 00-681 Warsaw, Poland*

³*UPMC Université Paris 06, Faculté de Physique, 4 place Jussieu, 75252 Paris Cedex 05, France*

(Received 12 September 2013; published 25 February 2014)

The study of the production of two forward jets with a large interval of rapidity at hadron colliders was proposed by Mueller and Navelet as a possible test of the high energy dynamics of QCD. We analyze this process within a complete next-to-leading logarithm framework, supplemented by the use of the Brodsky-Lepage-Mackenzie procedure extended to the perturbative Regge dynamics, to find the optimal renormalization scale. This leads to a very good description of the recent CMS data at LHC for the azimuthal correlations of the jets.

DOI: 10.1103/PhysRevLett.112.082003

PACS numbers: 12.38.Cy, 12.38.Qk, 13.85.Hd

Introduction.—Many processes have been proposed as a way to probe the high energy dynamics of QCD, described by the Balitsky-Fadin-Kuraev-Lipatov (BFKL) approach [1]. Among the most promising ones is the production of two forward jets separated by a large interval of rapidity at hadron colliders, proposed by Mueller and Navelet [2]. The purpose of the present Letter is to show that the most recent LHC data extracted by the CMS collaboration for the azimuthal correlations of these jets [3] are well described within this framework.

The description of this process involves two main building blocks: the jet vertex, which describes the transition from an incoming parton to a jet, and the Green's function, which describes the Pomeron exchange between the vertices. The first results of a complete next-to-leading logarithmic (NLL) calculation, including the NLL corrections both to the Green's function [4] and to the jet vertex [5], showed that the NLL corrections to the jet vertex have a very large effect, leading to a lower cross section and a much larger azimuthal correlation [6]. It was also observed that the results were very dependent on the choice of the scales, especially the renormalization scale μ_R and the factorization scale μ_F . This has been confirmed in a more recent study [7], where we used more realistic kinematic cuts. To reduce this dependency, we apply the physically motivated Brodsky-Lepage-Mackenzie (BLM) procedure [8] to fix the renormalization scale, as it was adapted to the resummed perturbation theory à la BFKL in Refs. [9].

Mueller-Navelet jets.—The observables which are of interest are the differential cross section C_0

$$C_0 = \frac{d\sigma}{d|\mathbf{k}_{J,1}|d|\mathbf{k}_{J,2}|dy_{J,1}dy_{J,2}}, \quad (1)$$

where $\mathbf{k}_{J,1}$, $\mathbf{k}_{J,2}$ are the transverse momenta of the jets and $y_{J,1}$, $y_{J,2}$ are their rapidities, and the azimuthal correlations [10] of the jets

$$\frac{C_n}{C_0} = \langle \cos [n(\phi_{J,1} - \phi_{J,2} - \pi)] \rangle \equiv \langle \cos(n\varphi) \rangle, \quad (2)$$

where $\phi_{J,1}$, $\phi_{J,2}$ are the azimuthal angles of the two jets. The relative azimuthal angle φ is defined such that $\varphi = 0$ corresponds to the back-to-back configuration.

The coefficients C_n can be expressed as

$$C_n = (4 - 3\delta_{n,0}) \int d(\text{P.S}) f(x_1) f(x_2) E_{n,\nu}(\mathbf{k}_1) E_{n,\nu}^*(\mathbf{k}_2) \times V(\mathbf{k}_1, x_1) V(\mathbf{k}_2, x_2) \cos(n\phi_{J,2}) \cos(n\phi_{J,1}) e^{\omega(n,\nu)Y}, \quad (3)$$

where $Y = y_{J,1} - y_{J,2}$ and we have defined for brevity the integration over the phase space and over the parameter ν of conformal weight as

$$\int d(\text{P.S}) = \int d\nu d\phi_{J,1} d^2\mathbf{k}_1 dx_1 d\phi_{J,2} d^2\mathbf{k}_2 dx_2, \quad (4)$$

where ν is integrated from $-\infty$ to $+\infty$, $x_{1(2)}$ is integrated from 0 to 1, and $\phi_{J,1(2)}$ is integrated from 0 to 2π ; f are the usual parton distribution functions (PDFs) and $E_{n,\nu}$ are the leading logarithmic (LL) BFKL eigenfunctions $E_{n,\nu}(\mathbf{k}_i) = (1/\pi\sqrt{2})(\mathbf{k}_i^2)^{\nu-(1/2)} e^{in\phi_i}$. The LL jet vertex reads

$$V_a^{(0)}(\mathbf{k}, x) = \frac{\alpha_s}{\sqrt{2}} \frac{C_{A/F}}{\mathbf{k}^2} \delta\left(1 - \frac{x_J}{x}\right) |\mathbf{k}_J| \delta^{(2)}(\mathbf{k} - \mathbf{k}_J), \quad (5)$$

where $C_A = N_c = 3$ and $C_F = (N_c^2 - 1)/(2N_c) = 4/3$ are to be used in the case of an incoming gluon and quark, respectively. The jet vertex V at NLL accuracy can be written as $V_a(\mathbf{k}, x) = V_a^{(0)}(\mathbf{k}, x) + \alpha_s V_a^{(1)}(\mathbf{k}, x)$. The expression of $V_a^{(1)}$, which has been recently reobtained in Ref. [11], can be found in Ref. [6]. Its expression in the limit of small cone jets has been computed in Ref. [12] and used in Refs. [13]. It was also rederived within the high energy effective action approach in Refs. [14].

At NLL, the eigenvalue of the BFKL kernel is [15–17]

$$\omega(n, \nu) = \bar{\alpha}_s \chi_0 \left(|n|, \frac{1}{2} + i\nu \right) + \bar{\alpha}_s^2 \tilde{\chi}_1 \left(|n|, \frac{1}{2} + i\nu \right), \quad (6)$$

where $\bar{\alpha}_s = N_c \alpha_s / \pi$,

$$\chi_0(n, \gamma) = 2\psi(1) - \psi\left(\gamma + \frac{n}{2}\right) - \psi\left(1 - \gamma + \frac{n}{2}\right), \quad (7)$$

with $\psi(x) = \Gamma'(x)/\Gamma(x)$,

$$\tilde{\chi}_1(n, \gamma) = \chi_1(n, \gamma) - \frac{\pi b_0}{N_c} \chi_0(n, \gamma) \ln \frac{|\mathbf{k}_{J,1}| \cdot |\mathbf{k}_{J,2}|}{\mu_R^2}, \quad (8)$$

where the expression for χ_1 , which was obtained in Refs. [15], can be found in Eq. (2.17) of Ref. [7].

BLM scale setting.—The BLM procedure is a way of absorbing the nonconformal terms of the perturbative series in a redefinition of the coupling constant, to improve the convergence of the perturbative series [18]. In practice, one should extract the β_0 -dependent part of an observable and choose the renormalization scale to make it vanish. The BLM procedure was first applied to BFKL dynamics in

Refs. [9] for the $\gamma^* \gamma^*$ total cross section, considering the NLL corrections to the Green's function but using the LL γ^* impact factor, with the important outcome of stabilizing the NLL BFKL intercept. This method was used in a similar spirit in Refs. [19]. We follow the same line of thought, taking into account the NLL corrections to the jet vertex.

In the expression of the coefficients C_n , the renormalization scale μ_R enters both ω (through α_s and the second term of $\tilde{\chi}_1$ which carries an explicit dependence on μ_R) and V . To separate the parts which depend on μ_R from those which do not, we rewrite Eq. (3) as

$$C_n = \alpha_s^2 (4 - 3\delta_{n,0}) \int d(\text{P.S}) D(\mathbf{k}_1, x_1) D(\mathbf{k}_2, x_2) \times A(x_1, \mathbf{k}_1, \phi_{J1}) A^*(x_2, \mathbf{k}_2, \phi_{J2}) e^{\omega(n, \nu) Y}, \quad (9)$$

where $A(x_i, \mathbf{k}_i, \phi_{Ji}) = f(x_i) E_{n, \nu}(\mathbf{k}_i) \cos(n\phi_{Ji})$. As $V^{(0)}$ and $V^{(1)}$ both contain a global α_s factor, we have defined $D^{(i)}(\mathbf{k}, x) = V^{(i)}(\mathbf{k}, x)/\alpha_s$ to make $D^{(0)}$ and $D^{(1)}$ α_s independent. We, now, focus on the μ_R -dependent part $D(\mathbf{k}_1, x_1) D(\mathbf{k}_2, x_2) e^{\omega(n, \nu) Y} \equiv B_n$ of Eq. (9). It can be expanded as the following series at NLL accuracy, for an arbitrary renormalization scale $\mu_{R, \text{init}}$

$$B_n = [D^{(0)}(\mathbf{k}_1, x_1) D^{(0)}(\mathbf{k}_2, x_2) + \alpha_s(\mu_{R, \text{init}}) (D^{(1)}(\mathbf{k}_1, x_1) D^{(0)}(\mathbf{k}_2, x_2) + D^{(0)}(\mathbf{k}_1, x_1) D^{(1)}(\mathbf{k}_2, x_2))] \times \sum_{m=0}^{\infty} \frac{(\bar{\alpha}_s(\mu_{R, \text{init}}) \chi_0(n, \gamma) Y)^m}{m!} \left(1 + m \bar{\alpha}_s(\mu_{R, \text{init}}) \frac{\tilde{\chi}_1(n, \gamma)}{\chi_0(n, \gamma)} \right). \quad (10)$$

Up to now, all the quantities we introduced were defined in the $\overline{\text{MS}}$ scheme. However, the BLM procedure is more conveniently applied in a physical renormalization scheme, so we first perform the transition from the modified minimal subtraction ($\overline{\text{MS}}$) scheme to the momentum subtraction (MOM) scheme, which is equivalent to writing [20]

$$\alpha_{\overline{\text{MS}}} = \alpha_{\text{MOM}} \left(1 + \alpha_{\text{MOM}} \frac{T_{\text{MOM}}}{\pi} \right), \quad (11)$$

where $T_{\text{MOM}} = T_{\text{MOM}}^\beta + T_{\text{MOM}}^{\text{conf}}$,

$$T_{\text{MOM}}^{\text{conf}} = \frac{N_c}{8} \left[\frac{17}{2} I + \frac{3}{2} (I-1) \xi + \left(1 - \frac{1}{3} I \right) \xi^2 - \frac{1}{6} \xi^3 \right],$$

$$T_{\text{MOM}}^\beta = -\frac{\beta_0}{2} \left(1 + \frac{2}{3} I \right), \quad (12)$$

where $\beta_0 = (11N_c - 2N_f)/3$, N_f is the number of flavors, $I = -2 \int_0^1 dx \ln(x)/[x^2 - x + 1] \approx 2.3439$, and ξ is a

gauge parameter. The variation of B_n when going from the $\overline{\text{MS}}$ to the MOM scheme is

$$\delta B_n = D^{(0)}(\mathbf{k}_1, x_1) D^{(0)}(\mathbf{k}_2, x_2) \bar{\alpha}_s(\mu_{R, \text{init}}) \frac{T_{\text{MOM}}}{N_c} \times \sum_{m=1}^{\infty} \frac{[\bar{\alpha}_s(\mu_{R, \text{init}}) \chi_0(n, \gamma) Y]^m}{(m-1)!}, \quad (13)$$

so that $B_{n, \text{MOM}} = B_n + \delta B_n$. To express $B_{n, \text{MOM}}$ as a function of an arbitrary renormalization scale μ_R we write $\alpha(\mu_{R, \text{init}})$ as

$$\alpha_s(\mu_{R, \text{init}}) = \alpha_s(\mu_R) \left(1 - \alpha_s(\mu_R) \frac{\beta_0}{4\pi} \ln \frac{\mu_{R, \text{init}}^2}{\mu_R^2} \right). \quad (14)$$

Now, we shall insert Eq. (14) in the expression of $B_{n, \text{MOM}}$ and extract the β_0 -dependent part. One can see from the expression of $V_a^{(1)}$ given in [6] that the term which depends on β_0 is proportional to the leading order part of the vertex, i.e., $D^{(1)\beta}(\mathbf{k}_i, x_i) = -(\beta_0/2\pi) \ln(|\mathbf{k}_i|/\mu_{R, \text{init}}) D^{(0)}(\mathbf{k}_i, x_i)$. Thus, the part of $B_{n, \text{MOM}}$ proportional to β_0 reads

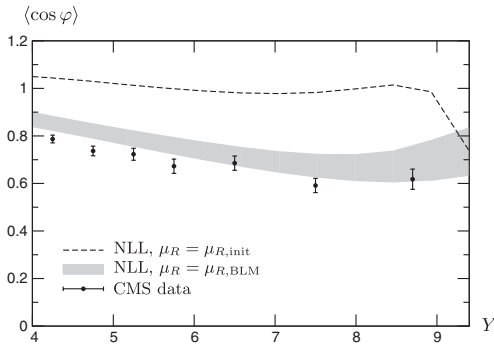


FIG. 1. Variation of $\langle \cos \varphi \rangle$ as a function of Y at NLL accuracy compared with CMS data.

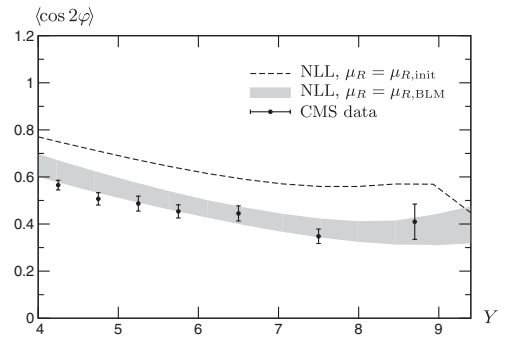


FIG. 2. Variation of $\langle \cos 2\varphi \rangle$ as a function of Y at NLL accuracy compared with CMS data.

$$B_{n,MOM}^\beta = D^{(0)}(\mathbf{k}_1, x_1) D^{(0)}(\mathbf{k}_2, x_2) \sum_{m=0}^{\infty} \alpha_s(\mu_R)^{m+1} \chi_0(n, \gamma)^m \left(\frac{YN_c}{\pi} \right)^m \frac{1}{m!} \left[-\frac{\beta_0}{2\pi} \ln \frac{|\mathbf{k}_1| \cdot |\mathbf{k}_2|}{\mu_{R,init}^2} \right. \\ \left. + m \frac{N_c}{\pi} \left(\frac{\tilde{\chi}_1^\beta(n, \gamma)}{\chi_0(n, \gamma)} + \frac{T_{MOM}^\beta}{N_c} \right) - m \frac{\beta_0}{4\pi} \ln \frac{\mu_{R,init}^2}{\mu_R^2} \right], \quad (15)$$

where $\tilde{\chi}_1^\beta$ and T_{MOM}^β are the β_0 -dependent parts of $\tilde{\chi}_1$ and T_{MOM} , respectively. The optimal scale $\mu_{R,BLM}$ is the value of μ_R that makes the expression inside the brackets vanish. Taking into account the fact that our initial scale is $\mu_{R,init} = \sqrt{|\mathbf{k}_{J,1}| \cdot |\mathbf{k}_{J,2}|}$ and that $D^{(0)}(\mathbf{k}_i, x_i)$ contains a factor $\delta^{(2)}(\mathbf{k}_i - \mathbf{k}_{J,i})$ which will enforce $|\mathbf{k}_i| = |\mathbf{k}_{J,i}|$ after integrating over $d^2\mathbf{k}_i$, we need to solve the equation

$$\frac{N_c}{\pi} \left(\frac{\tilde{\chi}_1^\beta(n, \gamma)}{\chi_0(n, \gamma)} + \frac{T_{MOM}^\beta}{N_c} \right) - \frac{\beta_0}{4\pi} \ln \frac{|\mathbf{k}_{J,1}| \cdot |\mathbf{k}_{J,2}|}{\mu_{R,BLM}^2} = 0, \quad (16)$$

whose solution is

$$\mu_{R,BLM}^2 = |\mathbf{k}_{J,1}| \cdot |\mathbf{k}_{J,2}| \exp \left[\frac{1}{2} \chi_0(n, \gamma) - \frac{5}{3} + 2 \left(1 + \frac{2}{3} I \right) \right]. \quad (17)$$

Theoretical uncertainties.—Despite the fact that we have used the BLM procedure to fix the renormalization scale, several theoretical uncertainties remain.

First, the scale of the prefactor α_s^2 in Eq. (9) is not fixed in our implementation of the scale fixing procedure. To evaluate the corresponding uncertainty, we consider two cases, namely, either we take for this scale $\mu_{R,BLM}$ or $\mu_{R,init}$.

Second, our calculation involves the factorization scale μ_F which enters both the PDFs and the hard part. In principle, one should vary independently μ_R and μ_F . But, since the choice $\mu_R = \mu_F$ is made by all PDFs fitting collaborations we are aware of, one could argue that, for consistency, we should do the same. To estimate the reliability of our results, we did two evaluations: one with $\mu_F = \mu_R = \mu_{R,BLM}$ and one with the “natural” choice $\mu_F = \sqrt{|\mathbf{k}_{J,1}| \cdot |\mathbf{k}_{J,2}|}$. In both cases, we chose the single scale entering the PDFs as μ_F .

Third, several methods [21,22] have been proposed to improve the NLL BFKL Green’s function by imposing its compatibility with DGLAP [23] in the collinear limit. As in Ref. [7], we implemented scheme 3 of Ref. [21] and found that the effect of such collinear improvement was important for the cross section but much smaller than the two previous uncertainties for all the angular quantities we study here.

Results.—Recently, the CMS collaboration measured the azimuthal decorrelation of Mueller-Navelet jets at the LHC at a center of mass energy of 7 TeV [3]. Here, we compare our results using the BLM procedure to this measurement. The quantities we discussed in the previous sections were differential with respect to the transverse momenta $\mathbf{k}_{J,1}$, $\mathbf{k}_{J,2}$ and the rapidities $y_{J,1}$, $y_{J,2}$ of the jets. Here, we try to stay as close as possible to the configuration used in Ref. [3]: $y_{J,1}$ and $y_{J,2}$ run between 0 and 4.7 and we integrate $\mathbf{k}_{J,1}$ and $\mathbf{k}_{J,2}$ from 35 to 60 GeV. The CMS collaboration did not use an upper cut on the transverse momenta of the jets, but we have to do so for numerical

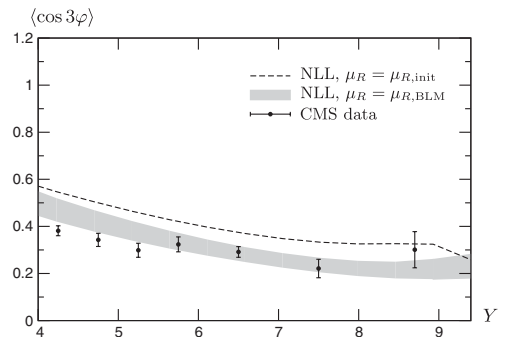


FIG. 3. Variation of $\langle \cos 3\varphi \rangle$ as a function of Y at NLL accuracy compared with CMS data.

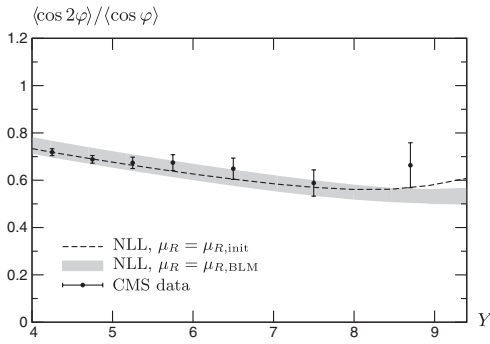


FIG. 4. Variation of $\langle \cos 2\varphi \rangle / \langle \cos \varphi \rangle$ as a function of Y at NLL accuracy compared with CMS data.

reasons. We have checked that our results do not depend strongly on the value of this cut, as the cross section is quickly decreasing with increasing transverse momenta. We use the anti- k_T jet algorithm [24] with a size parameter $R = 0.5$ and the MSTW 2008 PDFs [25]. The results displayed in every figure include the NLL BFKL calculation with the natural choice $\mu_R = \mu_F = \sqrt{|\mathbf{k}_{J,1}| \cdot |\mathbf{k}_{J,2}|}$ (dashed line), the NLL BFKL calculation with the BLM scale choice (gray uncertainty band) and the CMS data (dots with error bars). In our uncertainty band, we include the three effects discussed in the previous section.

Before comparing our results with data, we would like to note that our calculation is performed at the partonic level and does not include hadronization effects. However, the magnitude of these effects was estimated in [3] to be smaller than the experimental uncertainties, which justifies this comparison. We also did not take into account multiparton interactions, in which several partons from the same hadron take part in the interaction, as there is, for now, no theoretical framework to deal with such contributions at small x .

We first show results for the angular correlations $\langle \cos \varphi \rangle$, $\langle \cos 2\varphi \rangle$, and $\langle \cos 3\varphi \rangle$ as a function of the relative rapidity $Y = y_{J,1} - y_{J,2}$ on Figs. 1, 2, and 3, respectively. The conclusion for these three observables is similar: when one uses the natural scale, the NLL BFKL calculation is always above the data. But these data are much better described when setting the scale according to the BLM procedure.

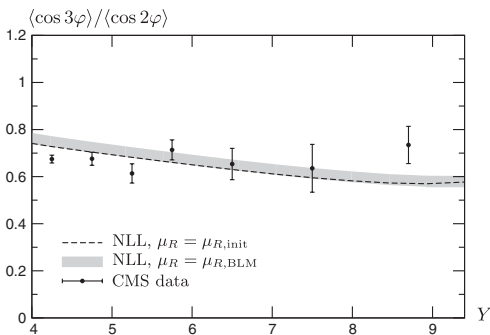


FIG. 5. Variation of $\langle \cos 3\varphi \rangle / \langle \cos 2\varphi \rangle$ as a function of Y at NLL accuracy compared with CMS data.

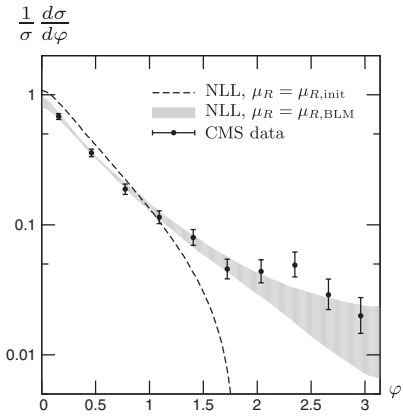


FIG. 6. Azimuthal distribution at NLL accuracy compared with CMS data.

On the other hand, the ratios $\langle \cos 2\varphi \rangle / \langle \cos \varphi \rangle$ and $\langle \cos 3\varphi \rangle / \langle \cos 2\varphi \rangle$ are almost not affected by the BLM procedure (see Figs. 4 and 5). This is because these observables are very stable with respect to the scales, as was noticed before in Refs. [6,7,17].

Another interesting observable, measured in Ref. [3], is the azimuthal distribution of the jets $(1/\sigma)(d\sigma/d\varphi)$, which can be expressed as

$$\frac{1}{\sigma} \frac{d\sigma}{d\varphi} = \frac{1}{2\pi} \left\{ 1 + 2 \sum_{n=1}^{\infty} \cos(n\varphi) \langle \cos(n\varphi) \rangle \right\}. \quad (18)$$

In Fig. 6, we show the comparison of our calculation with the data for the azimuthal distribution integrated over the range $6.0 < Y < 9.4$. We observe that using the natural scale $\mu = \sqrt{|\mathbf{k}_{J,1}| \cdot |\mathbf{k}_{J,2}|}$, the BFKL calculation is slightly above the data for $\varphi \lesssim 1$ and then becomes much lower than the data, even reaching negative values for $\varphi \sim \pi$. This issue does not arise when using BLM, and the agreement with data then becomes very good over the full φ range.

Comparison with the fixed order.—Since the CMS collaboration considered configurations with identical lower cuts on the jets transverse momenta, which would lead to unreliable results in a fixed-order treatment [26], a direct comparison of our analysis with this approach cannot

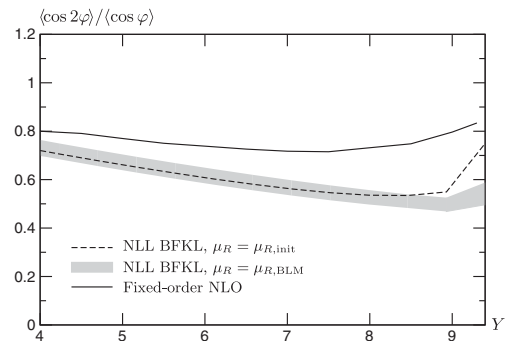


FIG. 7. Variation of $\langle \cos 2\varphi \rangle / \langle \cos \varphi \rangle$ as a function of Y at NLL accuracy compared with a fixed order treatment.

be performed. In Fig. 7, we show the comparison of our BFKL calculation with the results obtained with the NLO fixed-order code DIJET [27] for the ratio $\langle \cos 2\varphi \rangle / \langle \cos \varphi \rangle$ in the same kinematics as for previous results, but with the requirement that at least one jet has a transverse momentum larger than 50 GeV. As in [7], we see that there is a clear difference between BFKL and the fixed order, so we expect that an experimental analysis in an asymmetric configuration would discriminate between these approaches.

Energy-momentum conservation.—A general weakness of BFKL calculations is the absence of strict energy-momentum conservation. This has been studied for Mueller-Navelet jets in the past [28,29], using the leading order jet vertex. These studies showed that this is mainly an issue when $\mathbf{k}_{J,1}$ and $\mathbf{k}_{J,2}$ are different. This effect should not be dramatic here, as we use the same lower cut on these variables when comparing with CMS data, and the cross section decreases quickly with increasing $\mathbf{k}_{J,1}$, $\mathbf{k}_{J,2}$. Also, we expect that the inclusion of the NLL corrections to the jet vertex improves the situation.

Conclusions.—In this Letter, we have studied the azimuthal correlations of Mueller-Navelet jets and compared the predictions of a full NLL BFKL calculation with data taken at the LHC. We have shown that using the BLM procedure to fix the renormalization scale leads to a very good agreement with the data, much better than when using the natural value $\sqrt{|\mathbf{k}_{J,1}| \cdot |\mathbf{k}_{J,2}|}$.

We thank François Gelis and Edmond Iancu for warm hospitality at IPHT Saclay. We thank Michel Fontannaz, Grzegorz Brona, Hannes Jung, Victor Kim, and the Low-x 2013 Workshop participants for stimulating discussions. This work is supported by the French Grant PEPS-PTI PHENO-DIFF, the Polish Grant NCN No. DEC-2011/01/B/ST2/03915 and the Joint Research Activity Study of Strongly Interacting Matter (HadronPhysics3, Grant Agreement No. 283286) under the 7th Framework Programme of the European Community.

[1] V. S. Fadin, E. A. Kuraev, and L. N. Lipatov, *Phys. Lett.* **60B**, 50 (1975); E. A. Kuraev, L. N. Lipatov, and V. S. Fadin, *Sov. Phys. JETP* **44**, 443 (1976); **45**, 199 (1977); I. I. Balitsky and L. N. Lipatov, *Sov. J. Nucl. Phys.* **28**, 822 (1978).
 [2] A. H. Mueller and H. Navelet, *Nucl. Phys.* **B282**, 727 (1987).
 [3] CMS Collaboration, Report No. CMS-PAS-FSQ-12-002, 2013, <http://cds.cern.ch/record/1547075>.
 [4] V. S. Fadin and L. N. Lipatov, *Phys. Lett. B* **429**, 127 (1998); M. Ciafaloni and G. Camici, *Phys. Lett. B* **430**, 349 (1998).
 [5] J. Bartels, D. Colferai, and G. P. Vacca, *Eur. Phys. J. C* **24**, 83 (2002); **29**, 235 (2003).
 [6] D. Colferai, F. Schwennsen, L. Szymanowski, and S. Wallon, *J. High Energy Phys.* **12** (2010) 026.
 [7] B. Ducloué, L. Szymanowski, and S. Wallon, *J. High Energy Phys.* **05** (2013) 096.
 [8] S. J. Brodsky, G. P. Lepage, and P. B. Mackenzie, *Phys. Rev. D* **28**, 228 (1983).

[9] S. J. Brodsky, V. S. Fadin, V. T. Kim, L. N. Lipatov, and G. B. Pivovarov, *JETP Lett.* **70**, 155 (1999); **76**, 249 (2002).
 [10] V. Del Duca and C. R. Schmidt, *Phys. Rev. D* **49**, 4510 (1994); W. J. Stirling, *Nucl. Phys.* **B423**, 56 (1994).
 [11] F. Caporale, D. Y. Ivanov, B. Murdaca, A. Papa, and A. Perri, *J. High Energy Phys.* **02** (2012) 101.
 [12] D. Y. Ivanov and A. Papa, *J. High Energy Phys.* **05** (2012) 086.
 [13] F. Caporale, D. Y. Ivanov, B. Murdaca, and A. Papa, *Nucl. Phys.* **B877**, 73 (2013); F. Caporale, B. Murdaca, A. Sabio Vera, and C. Salas, *Nucl. Phys.* **B875**, 134 (2013).
 [14] M. Hentschinski and A. Sabio Vera, *Phys. Rev. D* **85**, 056006 (2012); G. Chachamis, M. Hentschinski, J. D. Madrigal Martinez, and A. Sabio Vera, *Phys. Rev. D* **87**, 076009 (2013).
 [15] A. V. Kotikov and L. N. Lipatov, *Nucl. Phys.* **B582**, 19 (2000); **B661**, 19 (2003).
 [16] D. Y. Ivanov and A. Papa, *Nucl. Phys.* **B732**, 183 (2006).
 [17] A. Sabio Vera, *Nucl. Phys.* **B746**, 1 (2006); A. Sabio Vera and F. Schwennsen, *Nucl. Phys.* **B776**, 170 (2007); F. Schwennsen Ph.D. thesis, DESY, 2007, [arXiv:hep-ph/0703198].
 [18] The BLM procedure was later extended to all orders, leading to the principle of maximal conformality [30].
 [19] M. Angioni, G. Chachamis, J. D. Madrigal Martinez, and A. Sabio Vera, *Phys. Rev. Lett.* **107**, 191601 (2011); M. Hentschinski, A. Sabio Vera, and C. Salas, *Phys. Rev. Lett.* **110**, 041601 (2013); *Phys. Rev. D* **87**, 076005 (2013).
 [20] W. Celmaster and R. J. Gonsalves, *Phys. Rev. Lett.* **42**, 1435 (1979); *Phys. Rev. D* **20**, 1420 (1979).
 [21] G. P. Salam, *J. High Energy Phys.* **07** (1998) 019.
 [22] M. Ciafaloni and D. Colferai, *Phys. Lett. B* **452**, 372 (1999); M. Ciafaloni, D. Colferai, and G. P. Salam, *Phys. Rev. D* **60**, 114036 (1999); M. Ciafaloni, D. Colferai, G. P. Salam, and A. M. Stasto, *Phys. Rev. D* **68**, 114003 (2003).
 [23] V. N. Gribov and L. N. Lipatov, *Sov. J. Nucl. Phys.* **15**, 438 (1972); L. N. Lipatov, *Sov. J. Nucl. Phys.* **20**, 94 (1975); G. Altarelli and G. Parisi, *Nucl. Phys.* **B126**, 298 (1977); Y. L. Dokshitzer, *Sov. Phys. JETP* **46**, 641 (1977).
 [24] M. Cacciari, G. P. Salam, and G. Soyez, *J. High Energy Phys.* **04** (2008), 063.
 [25] A. D. Martin, W. J. Stirling, R. S. Thorne, and G. Watt, *Eur. Phys. J. C* **63**, 189 (2009).
 [26] J. R. Andersen, V. Del Duca, S. Frixione, C. R. Schmidt, and W. J. Stirling, *J. High Energy Phys.* **02** (2001) 007; M. Fontannaz, J. P. Guillet, and G. Heinrich, *Eur. Phys. J. C* **22**, 303 (2001).
 [27] P. Aurenche, R. Basu, and M. Fontannaz, *Eur. Phys. J. C* **57**, 681 (2008).
 [28] L. H. Orr and W. J. Stirling, *Phys. Rev. D* **56**, 5875 (1997).
 [29] V. Del Duca and C. R. Schmidt, *Phys. Rev. D* **51**, 2150 (1995); C. Marquet and C. Royon, *Phys. Rev. D* **79**, 034028 (2009).
 [30] S. J. Brodsky and L. Di Giustino, *Phys. Rev. D* **86**, 085026 (2012); S. J. Brodsky and X.-G. Wu, *Phys. Rev. D* **85**, 034038 (2012); *Phys. Rev. D* **86**, 079903(E) (2012); *Phys. Rev. Lett.* **109**, 042002 (2012); *Phys. Rev. D* **85**, 114040 (2012); M. Mojaza, S. J. Brodsky, and X.-G. Wu, *Phys. Rev. Lett.* **110**, 192001 (2013); X.-G. Wu, S. J. Brodsky, and M. Mojaza, *Prog. Part. Nucl. Phys.* **72**, 44 (2013); S. J. Brodsky, M. Mojaza, and X.-G. Wu, *Phys. Rev. D* **89**, 014027 (2014); X.-C. Zheng, X.-G. Wu, S.-Q. Wang, J.-M. Shen, and Q.-L. Zhang, *J. High Energy Phys.* **10** (2013) 117.